

## Growth and characterization of LuAs films and nanostructures

E. M. Krivoy, H. P. Nair, A. M. Crook, S. Rahimi, S. J. Maddox et al.

Citation: *Appl. Phys. Lett.* **101**, 141910 (2012); doi: 10.1063/1.4757605

View online: <http://dx.doi.org/10.1063/1.4757605>

View Table of Contents: <http://apl.aip.org/resource/1/APPLAB/v101/i14>

Published by the [American Institute of Physics](#).

---

### Related Articles

Anomalous behavior of epitaxial indium nano-contacts on cadmium-zinc-telluride

*Appl. Phys. Lett.* **101**, 132108 (2012)

Tellurium-modified silicon nanowires with a large negative temperature coefficient of resistance

*Appl. Phys. Lett.* **101**, 133111 (2012)

The effects of energy transfer on the Er<sup>3+</sup> 1.54 $\mu$ m luminescence in nanostructured Y<sub>2</sub>O<sub>3</sub> thin films with heterogeneously distributed Yb<sup>3+</sup> and Er<sup>3+</sup> codopants

*J. Appl. Phys.* **112**, 063117 (2012)

Tapered and aperiodic silicon nanostructures with very low reflectance for solar hydrogen evolution

*Appl. Phys. Lett.* **101**, 133906 (2012)

Formation and cell translocation of carbon nanotube-fibrinogen protein corona

*Appl. Phys. Lett.* **101**, 133702 (2012)

---

### Additional information on *Appl. Phys. Lett.*

Journal Homepage: <http://apl.aip.org/>

Journal Information: [http://apl.aip.org/about/about\\_the\\_journal](http://apl.aip.org/about/about_the_journal)

Top downloads: [http://apl.aip.org/features/most\\_downloaded](http://apl.aip.org/features/most_downloaded)

Information for Authors: <http://apl.aip.org/authors>

## ADVERTISEMENT



**Goodfellow**  
metals • ceramics • polymers • composites  
70,000 products  
450 different materials  
**small quantities fast**

[www.goodfellowusa.com](http://www.goodfellowusa.com)

## Growth and characterization of LuAs films and nanostructures

E. M. Krivoy,<sup>a)</sup> H. P. Nair, A. M. Crook, S. Rahimi, S. J. Maddox, R. Salas, D. A. Ferrer, V. D. Dasika, D. Akinwande, and S. R. Bank

Microelectronics Research Center, University of Texas at Austin, Texas 78712, USA

(Received 1 July 2012; accepted 20 September 2012; published online 4 October 2012)

We report the growth and characterization of nearly lattice-matched LuAs/GaAs heterostructures. Electrical conductivity, optical transmission, and reflectivity measurements of epitaxial LuAs films indicate that LuAs is semimetallic, with a room-temperature resistivity of  $90 \mu\Omega \text{ cm}$ . Cross-sectional transmission electron microscopy confirms that LuAs nucleates as self-assembled nanoparticles, which can be overgrown with high-quality GaAs. The growth and material properties are very similar to those of the more established ErAs/GaAs system; however, we observe important differences in the magnitude and wavelength of the peak optical transparency, making LuAs superior for certain device applications, particularly for thick epitaxially embedded Ohmic contacts that are transparent in the near-IR telecommunications window around  $1.3 \mu\text{m}$ . © 2012 American Institute of Physics. [<http://dx.doi.org/10.1063/1.4757605>]

Much attention has been given in recent years to rare-earth pnictide (RE-V) materials, particularly ErAs, which is the most heavily studied.<sup>1,2</sup> Many of the RE-Vs are rocksalt semimetals<sup>3–5</sup> and can be epitaxially integrated with III-V semiconductors as nanoparticles<sup>6</sup> and films.<sup>1</sup> This class of heterogeneous materials is often characterized by fast electron-hole recombination, reduced thermal conductivity, increased or decreased free carrier concentrations, and modified absorption spectra.<sup>7</sup> Applications for semimetallic nanostructures and films include thermoelectric devices,<sup>8</sup> plasmonic structures,<sup>9</sup> enhanced-conductivity tunnel junctions,<sup>10,11</sup> and epitaxially integrated Ohmic contacts.<sup>12</sup> Growth of these semimetallic materials can be performed within the normal growth window of III-V semiconductors, between  $\sim 400^\circ\text{C}$  and  $\sim 600^\circ\text{C}$ , making them attractive for the integration of epitaxially embedded semimetal layers and nanostructures into semiconductor devices. Prior studies of the growth of ErAs have yielded information about an embedded growth mode of the material system, where the erbium atoms displace the group-III atoms from the zincblende lattice and nucleate into rocksalt nanostructures that are 3–4 monolayer (ML) deep before coalescing laterally to form full films.<sup>13</sup> Because of the promising results from Er-V materials, it is of interest to explore the full range of the RE-Vs to develop materials systems spanning a range of III-V and group-IV substrate lattice parameters. Exchanging erbium for lutetium in the RE-As monopnictide, thereby altering the band structure and potentially the band alignments to III-V materials, has important implications for material characteristics, including free carrier concentration, resistivity, and optical properties. LuAs, being only 0.41% lattice-mismatched from GaAs, offers the potential for thick, coherent films, ideal for epitaxially embedded Ohmic contacts. When grown on the zinc-blende (100) GaAs, LuAs grows in the rock-salt crystal structure and has a single thermodynamically stable phase.<sup>14,15</sup> Additionally, as LuAs has a similar enthalpy of formation to that of ErAs,<sup>16</sup> growth is expected to be quite similar.

Previously, Taylor *et al.* used a vapor-solid reaction to synthesize LuAs to study its lattice parameter,<sup>17</sup> and Takagehara used the self-consistent augmented plane-wave method to calculate the LuAs electronic band structure.<sup>18</sup> Palmstrøm *et al.* grew the first epitaxial LuAs films on GaAs using molecular beam epitaxy (MBE);<sup>1</sup> however, its properties remain largely unexplored. Here we report the first growth and properties of thick,  $0.6 \mu\text{m}$ , LuAs films on GaAs, as well as of LuAs nanostructures embedded epitaxially in GaAs. We observe subtle, yet promising, differences in electrical, optical, and structural properties as compared with the more carefully studied ErAs/GaAs system, including a peak transparency window at  $\sim 1.3 \mu\text{m}$ . This, coupled with the inherent advantage that LuAs is the most closely lattice-matched RE-V binary to GaAs, makes LuAs compelling for further investigation, particularly for buried, epitaxial Ohmic contacts.

Samples were grown by solid-source molecular beam epitaxy in an EPI Mod. Gen. II system on semi-insulating (100) GaAs. The  $\text{As}_2$ :Ga beam equivalent pressure (BEP) ratio was 15:1, with  $\text{As}_2$ :Lu BEP ratios of 10:1 and 46:1 during the growth of films and nanostructures, respectively. 200 nm GaAs buffer layers were grown at a nominal substrate temperature of  $545^\circ\text{C}$ , with LuAs films grown at  $430^\circ\text{C}$ . The lower substrate temperature during LuAs growth was necessary to observe reflection high-energy electron diffraction (RHEED) intensity oscillations during the growth, which were employed to calibrate the growth rate of the material. Structural quality was assessed *in situ* with RHEED and *ex situ* with X-ray diffraction (XRD), dynamical secondary ion mass spectroscopy (SIMS), and transmission electron microscopy (TEM) to confirm the growth rate.

Thick films of LuAs on GaAs were grown first to explore LuAs as a potential replacement for ErAs as epitaxial, nearly lattice-matched, Ohmic contacts. An average room-temperature resistivity of  $90 \mu\Omega \text{ cm}$  was found for LuAs films of varying thicknesses, in agreement with the prior report by Palmstrøm *et al.* and comparable with values reported for ErAs ( $\sim 40\text{--}70 \mu\Omega \text{ cm}$ ).<sup>1,14</sup> Temperature-dependent resistivity measurements of a 10 ML LuAs film and of a 600 nm LuAs film capped with 10 nm of GaAs to

<sup>a)</sup>Electronic mail: erica.krivoy@mail.utexas.edu.

prevent oxidation, plotted in Fig. 1, show a variation in film resistivity over a temperature range of 77–297 K of <20% for the 10 ML film, and a  $\sim 2\times$  variation in the 600 nm film. This decrease in resistivity with decreasing temperature is consistent with semimetallic behavior. The difference in variation in the two films may be related to the influence of surface states in the thin film, which are much less influential in the bulk, 600 nm film. A (115) reciprocal space map, not shown, of the relaxed 0.6  $\mu\text{m}$  film of LuAs indicated a single crystalline layer and minimal distribution of the in-plane lattice constant, with an in-plane distribution full-width at half-maximum (FWHM) of <8000 ppm, and an out-of-plane FWHM of <4200 ppm for the LuAs peak. The residual strain observed in the LuAs thick film possibly results from the  $\sim 2\times$  difference in thermal expansion coefficients between the RE-V rocksalt film and the III-V zincblende substrate.<sup>19</sup> Fig. 2 plots the transmission spectra of a 0.6  $\mu\text{m}$  LuAs film and a comparably grown 0.5  $\mu\text{m}$  film of ErAs, each capped with 10 nm of GaAs. The transmission spectra are qualitatively similar; however, the most notable difference is a broader transmission window for LuAs, which includes the technologically important 1.3  $\mu\text{m}$  region.<sup>20</sup> Additionally, the peak transmission of the thicker LuAs film is 1.5 $\times$  that of the ErAs. The two attenuation valleys observed in the LuAs spectrum, which have also been observed in ErAs,<sup>20</sup> could possibly be attributed to splitting due to exchange interactions between the conduction band and the 4f shell electrons.<sup>4,21</sup> Shubnikov de Haas measurements on films of LuAs are in progress and may further elucidate the bandstructure of the material system.<sup>4</sup>

The combined properties of moderate resistivity and optical transparency at near-infrared wavelengths, as well as near lattice-matching, make LuAs films attractive for thick, transparent, epitaxial Ohmic contacts on GaAs, similar to those proposed by Hanson *et al.* for ErAs,<sup>20</sup> but with the advantage of superior lattice-matching and transparency. Additionally, because the band-to-band absorption peaks and Drude absorption edges observed in reflection measurements, shown in Fig. 3, occur at different spectral locations than other previously reported RE-V materials,<sup>20,22,23</sup> there

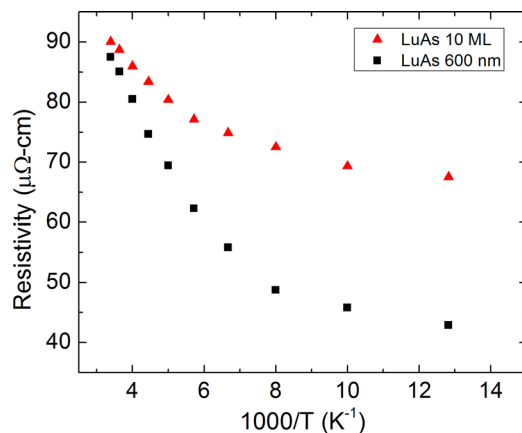


FIG. 1. Temperature-dependent resistivity of a 10 ML LuAs film and a 600 nm LuAs film normalized by their room-temperature resistivity. Resistivity variation of <20% from 77 K to 297 K is observed in the thin film, and  $\sim 2\times$  in the thick film. The negative temperature coefficient observed is consistent with semimetallic transport.

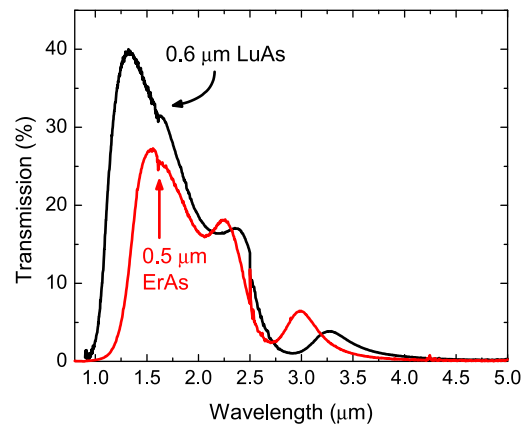


FIG. 2. Transmission spectra for a 0.6  $\mu\text{m}$  film of LuAs and a 0.5  $\mu\text{m}$  film of ErAs. The LuAs film exhibited superior transmission over the technologically important near-IR 1.3–1.55  $\mu\text{m}$  range, despite being 20% thicker. Absorption peaks were red-shifted to longer wavelengths by  $\sim 150$  nm in LuAs, as compared with ErAs.

are potential advantages for applying LuAs films to other photonic devices, including enhancement in absorption/emission due to the plasmon resonance.<sup>3</sup> The apparent Drude edge in the reflectivity spectrum, as well as the metal-like behavior of the temperature-dependent resistivity, suggests that LuAs is semimetallic, in agreement with earlier density functional theory (DFT) bandstructure calculations<sup>21,24,25</sup> and experimental observations by Palmstrøm *et al.*<sup>1</sup>

In addition to LuAs films, it is of interest to explore the properties of LuAs nanoparticles for application to tunneling enhancement<sup>10</sup> and fast photoconductors.<sup>26</sup> Here we report the first investigation into the growth and characterization of LuAs nanostructures. A multilayer stack of LuAs nanostructures was grown at 530  $^{\circ}\text{C}$  for cross-sectional TEM, shown in Fig. 4(a). LuAs deposition was progressively increased from 0.5 to 3.0 of equivalent MLs, following a comparable nucleation of nanostructures as studied in ErAs/GaAs by Kadow *et al.*<sup>27</sup> Each LuAs layer was capped with 50 nm of GaAs to establish the limits for LuAs nanostructure deposition while maintaining high-quality GaAs overgrowth.<sup>12</sup> RHEED was observed during the GaAs overgrowth at each stage of the multilayer stack to determine the amount of LuAs deposition that could not be overgrown with high-

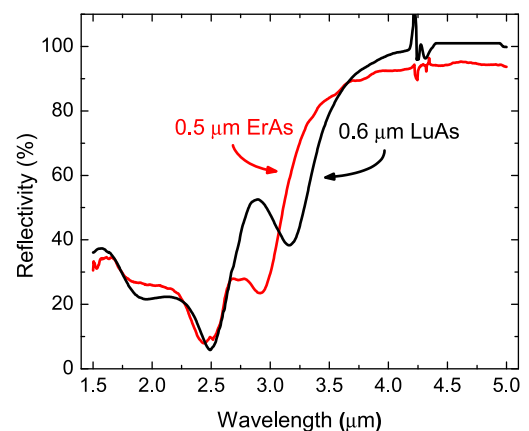


FIG. 3. Reflectivity spectra for a 0.6  $\mu\text{m}$  film of LuAs and a 0.5  $\mu\text{m}$  film of ErAs. A red-shift of  $\sim 250$  nm is evident in the Drude edge of the LuAs film, with respect to the ErAs film.

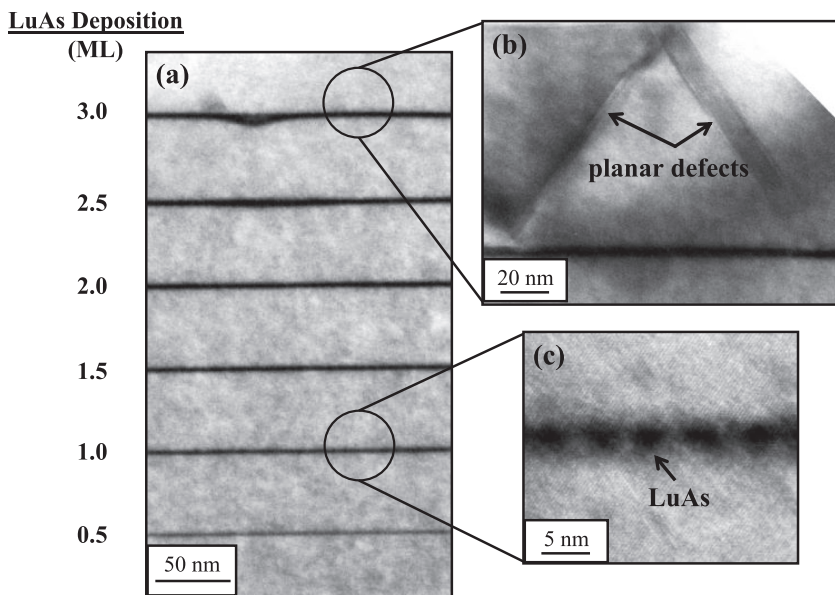


FIG. 4. Cross-sectional transmission electron microscopy (XTEM) images along (110) zone-axis of a LuAs/GaAs multilayer stack. (a) The complete multilayer structure, (b) planar defect formation following the 3.0 ML deposition of LuAs, (c) 1.0 ML deposition of LuAs nanoparticles.

quality GaAs, typically  $\sim 2$  ML for ErAs on GaAs.<sup>6</sup> Bright, streaky RHEED was observed during GaAs overgrowth of LuAs depositions, where a slight degradation of the RHEED pattern was noticeable for overgrowth of 2.5 ML of LuAs, and overgrowth of the 3.0 ML of LuAs was significantly degraded. As shown in Fig. 4(b), planar defect formation was evident in XTEM within the GaAs overgrowth of 3.0 MLs of LuAs. The similarities in the GaAs overgrowth of LuAs nanostructures with the ErAs/GaAs material system suggest that LuAs may be grown using the nanoparticle seeded embedded growth method as reported by Crook *et al.*,<sup>28</sup> meriting further investigation. A strong dependence on temperature and arsenic overpressure is observed in nanostructure size using plan-view TEM, as seen in Fig. 5. At higher depositions, nanostructures form into interconnected networks; this is observed in 1.8 ML deposition of LuAs, similar to what was observed by Kadow *et al.* in ErAs/GaAs.<sup>27</sup>

Given the similarity in bulk properties and growth morphology, the optical properties of LuAs nanostructures em-

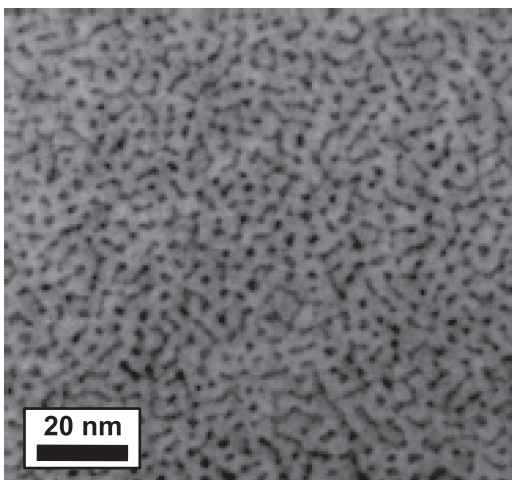


FIG. 5. Plan-view transmission electron microscopy image of a LuAs/GaAs multilayer stack, 1.8 ML LuAs/50 nm GaAs  $5\times$  repetition. Imaged sample 20–70 nm in thickness, potentially showing 1–2 nanoparticle layers.

bedded in GaAs are expected to be similar to those of ErAs/GaAs.<sup>9</sup> LuAs/GaAs superlattices were grown for absorption studies (Table I), keeping total epi-layer thickness constant at  $1\ \mu\text{m}$ , and a constant total volumetric deposition of LuAs. Transmission and reflection spectroscopy were performed on the samples to extract their absorption coefficient spectra. A red-shift of the absorption peaks with increasing LuAs deposition is evident in Fig. 6. The origin of this shift in the absorption spectrum is under investigation, with potential explanations ranging from shifts in a plasmon resonance<sup>9</sup> to increased quantum confinement with decreasing particle size.<sup>5,27</sup> The LuAs nanoparticle superlattices resulted in absorption spectra with relatively narrow linewidths even at longer wavelengths, showing minimal degradation of absorption strength with increasing deposition. Similarly grown ErAs superlattice structures exhibited the same relatively narrow linewidth and minimal degradation at longer wavelength. This is distinct from what has been previously reported by Hanson *et al.* in the ErAs/GaAs system, where significant spectral broadening was observed in superlattices with larger ErAs nanoparticles.<sup>9</sup> This may be attributed to subtle differences in growth technique; both substrate temperature and As:RE flux ratio are known to affect the particle morphology. Further investigations are underway into the resistivity and carrier lifetimes of LuAs nanoparticle superlattices for photomixer applications, as well as measurements of Schottky barrier heights of LuAs/GaAs, and will be reported subsequently.

In summary, the growth of epitaxial thick films and nanoparticles of LuAs was reported. LuAs appears to be semimetallic with comparable resistivity to ErAs, but with

TABLE I. Sample structures for LuAs and ErAs superlattice absorption studies.

Sample	LuAs deposition (ML)	GaAs deposition (nm)	Superlattice periods
A	0.25	5	200
B	0.5	10	100
C	1.0	20	50

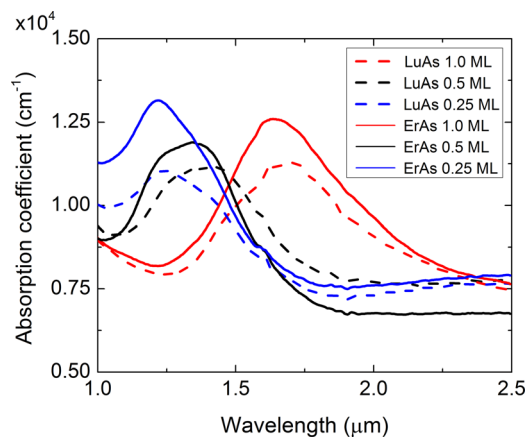


FIG. 6. Absorption spectra for LuAs superlattice structures (and similarly grown ErAs superlattice structures), each  $1\ \mu\text{m}$  total epi-layer thickness, with equal volumetric RE-As concentration. The absorption peak shifted to longer wavelengths for larger depositions, while maintaining a relatively narrow linewidth at longer wavelengths.

superior optical transmission characteristics in the near-IR, making LuAs films potentially attractive for transparent epitaxial Ohmic contacts. Other potential future applications include active plasmonic devices, photomixers, and nanoparticle-enhanced tunnel junctions lattice-matched to GaAs for photovoltaics. Future efforts should focus on incorporating LuAs films and nanostructures into optoelectronic devices.

This work was supported by ARO through the PECASE program (W911NF-09-1-0434) and monitored by Dr. Dwight Woolard, and AFOSR through the YIP (FA9550-10-1-0182) and by Dr. Kitt Reinhardt. This work was performed in part at the Microelectronics Research Center, a member of the National Nanotechnology Infrastructure Network (NNIN), supported by the National Science Foundation.

<sup>1</sup>C. J. Palmström, K. C. Garrison, S. Mounier, T. Sands, C. Schwartz, N. Tabatabaie, S. Allen, H. Gilchrist, and P. Miceli, *J. Vac. Sci. Technol. B* **7**, 747–752 (1989).

<sup>2</sup>L. E. Cassels, T. E. Buehl, P. G. Burke, C. J. Palmström, A. C. Gossard, G. Pernot, A. Shakouri, C. R. Haughn, M. F. Doty, and J. M. O. Zide, *J. Vac. Sci. Technol. B* **29**, 03C114 (2011).

- <sup>3</sup>E. R. Brown, A. Bacher, D. Driscoll, M. Hanson, C. Kadow, and A. C. Gossard, *Phys. Rev. Lett.* **90**, 077403 (2003).
- <sup>4</sup>S. J. Allen, Jr., F. DeRosa, C. J. Palmström, and A. Zrenner, *Phys. Rev. B* **43**, 9599 (1991).
- <sup>5</sup>J. Kawasaki, R. Timm, K. Delaney, E. Lundgren, A. Mikkelsen, and C. Palmström, *Phys. Rev. Lett.* **107**, 036806 (2011).
- <sup>6</sup>C. Kadow, S. B. Fleischer, J. P. Ibbetson, J. E. Bowers, A. C. Gossard, J. W. Dong, and C. J. Palmström, *Appl. Phys. Lett.* **75**, 3548 (1999).
- <sup>7</sup>M. P. Hanson, S. R. Bank, J. M. O. Zide, J. D. Zimmerman, and A. C. Gossard, *J. Cryst. Growth* **301–302**, 4 (2007).
- <sup>8</sup>X. Liu, A. T. Ramu, J. E. Bowers, C. J. Palmström, P. G. Burke, H. Lu, and A. C. Gossard, *J. Cryst. Growth* **316**, 56 (2011).
- <sup>9</sup>M. P. Hanson, A. C. Gossard, and E. R. Brown, *J. Appl. Phys.* **102**, 043112 (2007).
- <sup>10</sup>J. M. O. Zide, A. Kleiman-Shwarsctein, N. C. Strandwitz, J. D. Zimmerman, T. Steenblock-Smith, A. C. Gossard, A. Forman, A. Ivanovskaya, and G. D. Stucky, *Appl. Phys. Lett.* **88**, 162103 (2006).
- <sup>11</sup>P. Pohl, F. H. Renner, M. Eckardt, A. Schwanhauser, A. Friedrich, O. Yuksekdog, S. Malzer, G. H. Dohler, P. Kiesel, D. Driscoll, M. Hanson, and A. C. Gossard, *Appl. Phys. Lett.* **83**, 4035 (2003).
- <sup>12</sup>C. J. Palmström, *Annu. Rev. Mater. Sci.* **25**, 389 (1995).
- <sup>13</sup>B. D. Schultz, S. G. Choi, and C. J. Palmström, *Appl. Phys. Lett.* **88**, 243117 (2006).
- <sup>14</sup>T. Sands, C. J. Palmström, J. P. Harbison, V. G. Keramidis, N. Tabatabaie, T. L. Cheeks, R. Ramesh, and Y. Silberberg, *Mater. Sci. Rep.* **5**, 99 (1990).
- <sup>15</sup>K. Gschneidner and F. Calderwood, *J. Phase Equilib.* **7**, 274–276 (1986).
- <sup>16</sup>A. M. Mulokozi, *J. Less-Common Met.* **75**, 125 (1980).
- <sup>17</sup>J. B. Taylor, L. D. Calvert, J. G. Despault, E. J. Gabe, and J. J. Murray, *J. Less-Common Met.* **37**, 217 (1974).
- <sup>18</sup>K. Takegahara, *Physica B: Condens. Matter* **186–188**, 850 (1993).
- <sup>19</sup>L. J. Brillson, *Contacts to Semiconductors: Fundamentals and Technology*, 1st ed. (Noyes Publications, New Jersey, 1994).
- <sup>20</sup>M. P. Hanson, A. C. Gossard, and E. R. Brown, *Appl. Phys. Lett.* **89**, 111908 (2006).
- <sup>21</sup>C.-G. Duan, T. Komesu, H.-K. Jeong, C. N. Borca, W.-G. Yin, J. Liu, W. N. Mei, P. A. Dowmen, A. G. Petukhov, B. D. Schultz, and C. J. Palmström, *Surf. Rev. Lett.* **11**, 531 (2004).
- <sup>22</sup>M. P. Hanson, Erbium-V Semimetal and III-V Semiconductor Composite Materials, University of California, Santa Barbara, 2007.
- <sup>23</sup>M. Said, F. B. Zid, C. Bertoni, and S. Ossicini, *Eur. Phys. J. B: Condens. Matter Complex Syst.* **23**, 191–199 (2001).
- <sup>24</sup>A. G. Petukhov, W. R. L. Lambrecht, and B. Segall, *Phys. Rev. B* **53**, 4324 (1996).
- <sup>25</sup>L. Pourovskii, K. Delaney, C. van de Walle, N. Spaldin, and A. Georges, *Phys. Rev. Lett.* **102**, 096401 (2009).
- <sup>26</sup>D. C. Driscoll, M. P. Hanson, A. C. Gossard, and E. R. Brown, *Appl. Phys. Lett.* **86**, 051908 (2005).
- <sup>27</sup>C. Kadow, J. A. Johnson, K. Kolstad, J. P. Ibbetson, and A. C. Gossard, *J. Vac. Sci. Technol. B* **18**, 2197 (2000).
- <sup>28</sup>A. M. Crook, H. P. Nair, D. A. Ferrer, and S. R. Bank, *Appl. Phys. Lett.* **99**, 072120 (2011).